CRYSTAL GROWTH & DESIGN

Article

Metal-bound Nitrate Anion as an Acceptor for Halogen Bonds in mono-Halopyridine-Copper(II) nitrate Complexes

Rakesh Puttreddy, Anssi Peuronen, Manu Lahtinen, and Kari Rissanen

Cryst. Growth Des., **Just Accepted Manuscript** • DOI: 10.1021/acs.cgd.9b00284 • Publication Date (Web): 29 May 2019

Metal-bound Nitrate Anion as an Acceptor for Halogen Bonds in *mono*-Halopyridine-Copper(II) nitrate Complexes

Rakesh Puttreddy,[a] Anssi Peuronen,[b] Manu Lahtinen[a] and Kari Rissanen[a]*

[a]*University of Jyvaskyla, Department of Chemistry, Survontie 9 B 40014 Jyvaskyla, Finland*

[b]*Inorganic Materials Chemistry Research Group, Laboratory of Materials Chemistry and Chemical Analysis, Department of Chemistry, University of Turku, 20014 Turku, Finland*

ABSTRACT Fifteen *n*-halopyridine-$Cu(NO_3)_2$ complexes (*n* = 2, 3, 4) obtained from two different solvents, acetonitrile and ethanol, are investigated for C−X···O−N halogen bonds (XBs) in the solid-state by single and powder X-ray diffraction. The nitrate anions bind copper(II) *via* anisobidentate modes and one of three oxygens act as XB acceptor to halogens on the core pyridine rings. The N-metal coordination activates electron deficient π-system and triggers even C2- and C4-chlorines in the corresponding [Cu(2-chloropyridine)$_2$$(NO_3)_2$] and [Cu(4-chloropyridine)$_2$$(NO_3)_2$(ACN)] complexes to form short C–Cl2/Cl4···O−N halogen bonds. Notably, the C2–Cl2···O−N XBs with normalized XB distance parameter (R_{XB}) 0.89 is close to C2–I2···O−N XBs [R_{XB} = 0.88] in [Cu(2-

iodopyridine)$_2$(NO_3)$_2$] complex. In overall, the C–X···O–N halogen bonds in the studied complexes range from moderately short to roughly the vdW contact distance of the respective X···O atoms (R_{XB} = 0.88 - 0.99), and have a varying significance in governing the molecular packing respective of the complex. Among the studied complexes, two main coordination modes were observed – distorted octahedral and distorted pentagonal bipyramid – of which the latter results from the coordination of acetonitrile to the Cu(II) ion. The crystal structures showed that the steric bulk of C2-halogens in 2-halopyridines prevent this, while in similar conditions the 3- and 4-halopyridine ligands yield acetonitrile bound Cu(II)-complexes.

INTRODUCTION

Halogen bonding as a directional non-covalent interaction, parallel to hydrogen bonding, has been widely acknowledged as a valuable crystal engineering tool over the past few decades.[1–4] Within this period, perfluorinated aromatic/aliphatic molecules acting as halogen bond (XB) donors (*via* iodine/bromine), and organic molecules containing N/O/S-atom functioning as XB acceptors have become a popular way to construct and study XB based supramolecular systems[5] both in the solid-state and in solution.[6–8] Meanwhile, the use of halogen bonding to control molecular arrangements in metal coordination complexes has received much less attention even though interesting magnetic,[9,10] semiconductor[11,12] and luminescent properties,[13–15] have been reported to

such systems. One reason for the slow advent of XB related studies on metal complexes, wherein both the XB donor and acceptor moieties are in the same complex unit, most likely originates from the small set of easily accessible ligands for such studies. In this context, halopyridines are the most prevalent as they have been used as XB donors in [M(halopyridine)$_2$X$_2$] complexes wherein M–X···X'–C type XB interactions have been shown to exist.[16–18] The advantage of nitrogen-metal (N–M) coordination is that the consequent electron deficient π-system makes the covalently bound peripheral halogen atoms (C–X) of the halopyridines more electrophilic and thus enhances its XB donor capabilities.[19] This effect has been shown to vary in relation to the nature of the metal cation. Further altering of the XB donor properties of the halopyridines can be done by *e.g*. including additional halogen atoms at the ring.[20] In accordance with the latter strategy we have recently reported a solid-state investigation of series of [Cu(2,5-dihalopyridine)$_2$X$_2$] (X = Cl, Br) complexes in which C2- and C5-halogens act as XB donors toward Cu(II)-coordinated halides in C–X···X'–Cu fashion.[21,22]

Within the past few years, the number of studies that have contributed to the understanding of the XB interactions occurring in [M(halopyridine)$_2$X$_2$] complexes, where X is a metal-bound halide functioning as the XB acceptor, have increased. However, to the best of our knowledge, a very limited amount of systematic studies of XBs in halopyridine complexes have been conducted wherein the incorporated metal-bound counter anion is other than a halide species.[23] Our ongoing research of $^{-}$O–N^{+} acceptor-based halogen

bonded systems, where electronegative O-atom binds to an XB donor,[24–26] has led us to consider NO_3^- as an oxygen bearing anion suitable for such an investigations. Nitrate anion is well-known to engage in XB interactions through its O-atoms when suitable XB donor atoms are available.[27,28] As a counter anion, nitrate possesses versatile coordination abilities as it can display mono- bidentate-, and tridentate-coordination modes and can act as a bridge between metal centres.[29]

For the investigation of XB interactions in nitrate anion bearing halopyridine metal complexes, copper(II) were chosen as the metal cation which was already employed successfully in our previous studies.[22,30] For the study, all relevant mono-substituted halopyridines were used in the complexation reactions (**1**-**9**, Scheme1) in order to carry out a fully systematic study of the NO_3^-···X–C interactions occurring in the complexes formed. This comprehensive set of complexes gave an opportunity to investigate whether the selected donor-acceptors pairs are favourable partners in XB formation and how the chemical nature of the XB donor atom species (Cl/Br/I) as well as its position in the pyridine ring may affect the NO_3^-···X–C halogen bonding interactions. The complexations were carried out in two different solvents, acetonitrile (ACN) and ethanol (EtOH), both of which are known to coordinate to Cu(II) centres and thereby have the potential to amend the coordination geometries of copper(II). Moreover, both ACN and EtOH can themselves act as XB acceptors. Ethanol is also a hydrogen bond (HB) donor/acceptor which increases

the chance of inclusion of solvent in the crystal lattice of the complexes and the competition between XB and HB interactions.

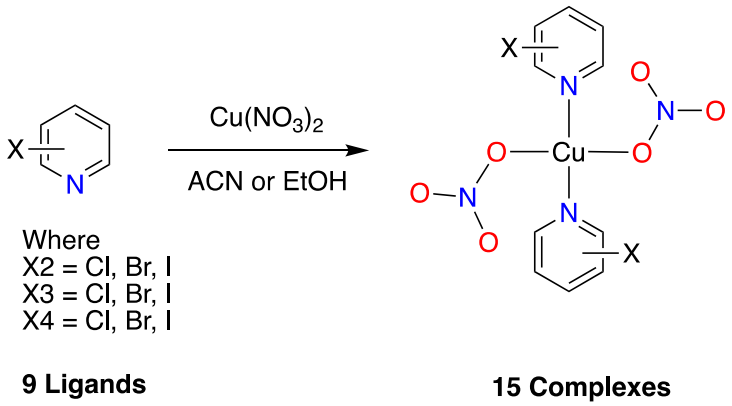

Scheme 1. Synthesis route to prepare [Cu^{II}(*n*-halopyridine)$_2$(NO_3)$_2$] complexes.

RESULTS AND DISCUSSION

The complexes were synthesized by mixing 1:1 and 2:1 molar ratio of halopyridines (**1** - **9**, Figure 1) and $Cu(NO_3)_2{\cdot}3H_2O$ in ACN or EtOH at room temperature (See Experimental Section for more details). Slow evaporation of the resulting blue coloured solutions afforded single crystals suitable for X-ray diffraction analysis. In addition, to determine the structural correlation between the measured single crystals and the crystalline bulk powders, powder X-ray diffraction (PXRD) data of each crystallization sample (when applicable) was collected and indexed by Pawley whole-pattern fitting method using the unit cell parameters of the corresponding single crystal structures as a starting point (see Supporting Information, for PXRD data). The single crystal structures and their relations to different mixing ratios and solvent conditions are all summarized in Table 1, where the

complexes of ligands **1** - **9** are indicated with a letter "**a**" or "**b**" depending on whether one or two structurally different Cu(II)-complexes were obtained per crystallization conditions. Complex crystals were obtained in both solvents with two different stoichiometry for all *n*-halopyridines except of ligand **7** that resulted only bulk powder in EtOH with 1:1 ratio.[31] It can be noted that PXRD analysis of the bulk suggests that aforesaid reaction product is structurally similar to **7b**.

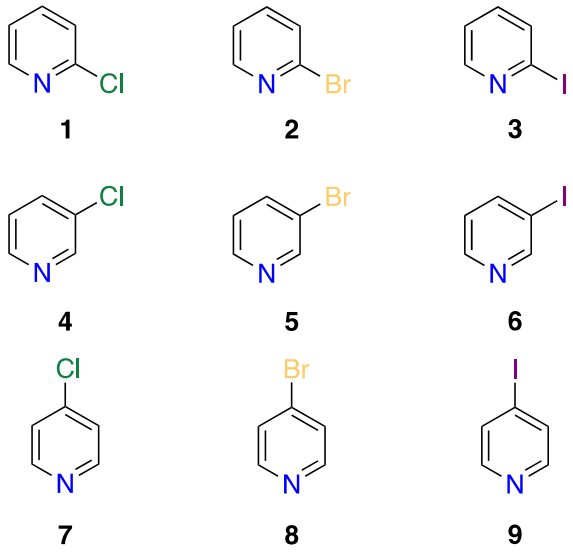

Figure 1. Molecular structures of halopyridines: 2-chloropyridine **1**), 2-bromopyridine **2**), 2-iodopyridine **3**), 3-chloropyridine **4**), 3-bromopyridine **5**), 3-iodopyridine **6**), 4-chloropyridine **7**), 4-bromopyridine **8**) and 4-iodopyridine **9**).

Table 1. Crystallization experiments of [Cu(*n*-halopyridine)$_2$(NO$_3$)$_2$] complexes made in acetonitrile (ACN) and ethanol (EtOH) with different *n*-halopyridine:Cu(NO$_3$)$_2$ molar ratios.

Solvent	ACN		EtOH	
Ligand	Stoichiometry L:Cu(NO$_3$)$_2$			
	1:1	2:1	1:1	2:1
1	**1a**	**1a**	**1a**	**1b**
2	**2a**	**2b**	**2a**	**2a**
3	**3a**	**3a**	**3a**	**3a**
4	**4a** (s)	**4a** (s)	**4b**	**4b**
5	**5a** (s)	**5a** (s)	**5b**	**5b**
6	**6a** (p)	**6a** (p)	**6a** (p)	**6a** (p)
7	**7a** (s)	**7a** (s)	**7b**♀	**7b**
8	**8a** (s)	**8a** (s)	**8b**	**8b**
9	**9a** (s)	**9a** (s)	**9b** (s)	**9b** (s)

s = Solvate; p = 1-D Polymeric structure; ♀characterized by PXRD

As shown in the Table 1, ligands (**1** - **9**) afforded two structurally different complexes displaying either polymorphism (**1** and **2**) or solvent inclusion into the Cu(II) coordination sphere (**4**, **5**, **7** - **9**). Only one ligand falls in neither of the two categories, but instead yields a polymeric complex (**6a**) wherein bridging nitrate anions constitute a 1-D network structure. With ligands **4**, **5**, **7** and **8**, the solvent bound complexes are formed only in the ACN whereas ligand **9** yielded a complex in which EtOH is coordinated to the Cu(II)-centre. It is noteworthy to mention that none of the crystal structures have solvent accessible voids, thus lacking non-coordinated ACN or EtOH molecules.

Coordination geometry analysis

Before an in-depth analysis of the XBs and other intermolecular interactions that contribute to the crystal packing in the studied systems, we would like to discuss some of the overall aspects of the coordination geometries in the complexes. The solvent free monomeric complexes comprise of two halopyridines and two nitrate anions coordinating to a single Cu(II)-centre. The nitrate ligands are coordinated in anisobidentate fashion to the Cu(II) thereby creating a distorted octahedral coordination environment along with the halopyridine ligands.[32,33] The asymmetric nature of the Cu–O_2N bonds between Cu(II) centre and single nitrate anion varies significantly between different Cu(II)-complexes and falls roughly in the range of 0.22 - 0.64 Å. For the solvated systems, solvent molecule is directly coordinated to the Cu(II)-centre along with two nitrates and two halopyridines thereby transforming the distorted octahedral to distorted pentagonal bipyramid geometry – a coordination geometry frequently reported for Cu(II)-complexes.[34–38] In the only polymeric complex **6a**, two Cu(II) centres are bridged by two nitrates *via* one O-atom of each of the nitrates. The identical (by symmetry) distorted octahedral coordination geometry of each of these two Cu(II)-centres is completed by another anisobidentate-fashion coordinated nitrate, along with two 3-iodopyridines. The polymeric 1D-continuity is obtained by one of the two connecting O-atoms of each of the latter two nitrates acting as bridges to adjacent, structurally different Cu(II)-centres.

The nitrate anion conformations in the studied monomeric complexes can be further classified into three main types. Complex **2a** together with two computational models are used as examples to present the conformational modes in Figure 2. When both O*-atoms (O-atoms with longer N–O···Cu contacts) are at *anti*-position to *syn*-positioned C2-bromines, the nitrate anion is defined to be in *syn*-mode (Figure 2a). In *syn*'-mode the C2-bromines and the nitrate anions (Figure 2c) occupy the same side (*syn*-*syn*-mode) whereas in the intermediate conformation, *i.e. anti*-mode, O*-atoms lie on opposite sides (Figure 2b). In the studied systems, *syn*-mode is the most common nitrate conformation and is displayed by all 2-halopyridine complexes (expect of the one of the two distinct complex units in **2b**; *vide infra*) and solvent adducts of 3- and 4-halopyridine complexes. In 2-halopyridine complexes the occurrence of *syn*-mode can be explained by the steric hindrance between the nitrate oxygens and bulky C2-halogens (also at *syn*-positions relative to each other) which also prohibits the coordination of additional solvents to the Cu(II)-ion. In structures, where solvent is coordinated to the Cu(II) the *syn*-inducing steric effect comes from the solvent-nitrate repulsion. Intramolecular interactions, such as the formation of $(C–X)_2$···O–N XBs, may further promote the *syn*-conformation. In the absence of intramolecular ligand-ligand steric effects (solvent free 3- and 4-halopyridine complexes) the observed nitrates are always in *anti*-conformation. The *syn*'-conformation is not observed within the studied systems.

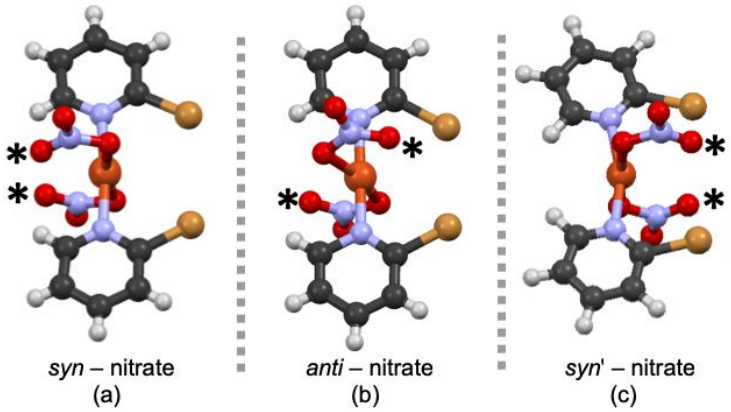

Figure 2. Three [Cu(2-bromopyridine)$_2$(NO_3)$_2$] complexes which illustrate the conformations of nitrate anions: a) *syn*-mode in complex **2a**, b) *anti*-, and c) *syn*'-modes showed in model structures made using Spartan software (B3LYP/6-31G* level of theory). Note: Oxygens marked with '*' represent elongated Cu–O contacts, which are not drawn for viewing clarity.

Analysis of non-covalent interactions

Structural analysis of the determined crystal structures revealed different intermolecular interactions and molecular packing schemes that will be interpreted in the following chapters with particular emphasize on XB interactions. The bond parameters for various XB contacts existing in the complexes are shown in the Table 2. In addition to X···O bond distances, the normalized XB distance parameters, R_{XB}, are also presented for giving a coarse estimation of the XB strengths. The R_{XB} is defined as $R_{XB} = d_{XB}/X_{vdW}+B_{vdW}$, where d_{XB} [Å] is the distance between the donor atom (X) and the acceptor atom (B), and X_{vdW} and B_{vdW} the van der Waal radii [Å] of X and B, respectively. The packing index (PI) parameters (for **1a** – **9b**) are

calculated using the PLATON program[39] and are also listed in Table 2. The PI represents the volume taken up by the molecules/ions in the crystal lattice and thus provides information on the intermolecular interactions in the solid-state.

Table 2. XB bond and packing index parameters for complexes **1a** – **9b**.

Complex	Packing Index	Motif	*d* (X···O), Å	∠C–X···O (°)	R_{XB}
1a	70.7	C2c–Cl2c···O3a	2.908(6)	155.1	0.89
1b	70.8	--[a]	--[a]	--[a]	--[a]
2a	71.9	C2–Br2···O3'	3.182(5)	174.0	0.94
		C2a–Br2a···O3a'	3.043(5)	172.7	0.90
2b	70.7	C2–Br2···O2c	3.16(1)	170.3	0.94
		C2a–Br2a···O2c	3.106(8)	169.5	0.92
3a	71.9	C2–I2···O3'	3.082(3)	177.2	0.88

4a	70.6	--[a]	--[a]	--[a]	--[a]
4b	72.7	--[a]	--[a]	--[a]	--[a]
5a	70.5	C3–Br3···O1"	3.229(2)	155.2	0.96
5b	73.2	C3–Br3···O2'	3.297(8)	153.2	0.98
6a	71.8	C3a–I3a···O2b'	3.055(3)	168.0	0.87
		C3b–I3b···O2a'	3.219(3)	175.6	0.92
		C3'–I3'···O2'	3.467(3)	176.5	0.99
7a	70.0	C4–Cl4···O2a'	3.036(3)	177.1	0.93
		C4a'–Cl4a'···O2	3.076(3)	170.3	0.94
7b	73.5	C4–Cl4···O2'	3.138(4)	170.0	0.96
		C4a–Cl4a···O2a'	3.191(4)	173.3	0.98
8a	70.1	C4–Br4···O2a'	3.030(4)	175.7	0.98
		C4a'–Br4a'···O2	3.071(4)	168.8	0.91
8b	73.8	C4–Br4···O2'	3.105(7)	170.0	0.92
		C4a–Br4a···O2a'	3.131(8)	173.4	0.93
9a	69.4	C4–I4···O2a'	3.086(4)	173.9	0.88
		C4a'–I4a'···O2	3.128(4)	167.9	0.89
9b	69.6	C4–I4···O2'	3.153(3)	172.9	0.90
		C4a–I4a···O2a'	3.028(3)	171.9	0.87

[a] The halogen substituents are XB passive.

Of the two polymorphs obtained with ligand **1**, complex **1a** crystallizes in triclinic crystal system *P*-1 and has two crystallographically independent [Cu(2-chloropyridine)$_2$(NO$_3$)$_2$] complexes in the asymmetric unit. The four distinct 2-chloropyridine moieties have only one C2-chlorine (Cl2c) engaged in XB interactions (XB active). As expected, the favoured XB acceptor is an O-atom of the nitrate anion (O3a) which along with the chloride donor atom forms a notably short XB (R_{XB} = 0.89; Figure 3a). However, it must be reminded that

a short contact distance does not necessarily correlate directly to the strength of the XB. If that would be the case, it is expect some of the other three equally potential XB donors in the structure could also participate in halogen bonds. In contrast, C2–Cl2 exhibits type I halogen-halogen[40] contact [C2–Cl2···Cl2'–C2', *d*(Cl2···Cl2') = 3.305(3) Å; Figure 3a] whereas the remaining two chlorines are XB passive (Cl2a and Cl2b). Rather than by XBs, the molecular packing seems to be dictated by NO_3^-···H–C interactions as these contacts exist in multitude between the adjacent Cu(II)-complex units.

Polymorphic structure **1b** crystallizes in the triclinic *P*-1 system, similarly to **1a**, but in a unit cell half its size. Therefore, its asymmetric unit contains only a single [Cu(2-chloropyridine)$_2$(NO_3)$_2$] unit in which both C2-chlorines are XB passive. The molecular packing is governed by NO_3^-···H–C interactions, weak C2–Cl2···H–C hydrogen bonds, π-π interactions (C2–Cl2···π) and anion-π interactions [*d*(N2–O2···π(C2')) = 3.101(6) Å][41] as illustrated in Figure 3b.

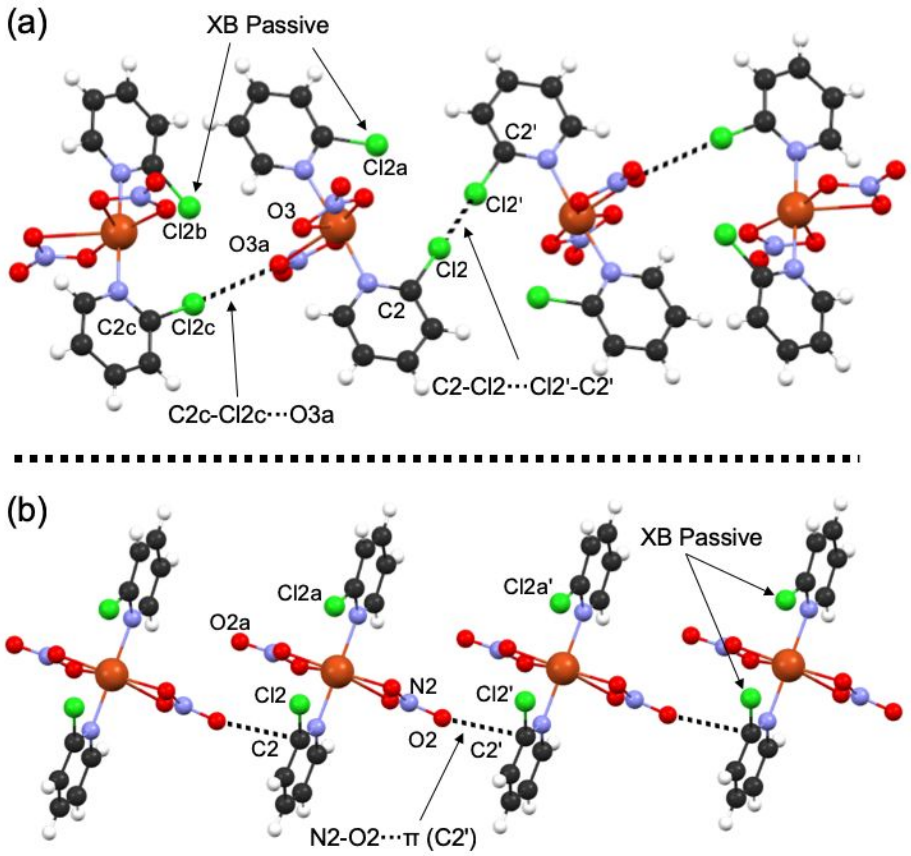

Figure 3. Partial view of molecular packing in crystal structures of complexes a) **1a** and b) **1b**. Selected atoms are numbered for the viewing clarity. Atoms labelled with Cl2' in **1a** and **1b** were generated by using symmetry operators 1-x, -y, 2-z and -1+x, y, z, respectively.

In the case of 2-bromopyridine (**2**), two polymorphs are obtained. Complex **2a** crystallizes in orthorhombic crystal system ($Pca2_1$) with a single molecule in its asymmetric unit. The complexes are ordered to infinite XB-mediated 1-D rows along the *b*-axis with two crystallographically distinct C–Br···O–N interactions (R_{XB} = 0.94, R_{XB} = 0.90) as shown in Figure 4a. The R_{XB} values for complex **2a** with C2-bromines are somewhat higher than in

complex **1a** with C2-chlorine substituents. However, the C–Br···O–N XBs are significantly more linear (*ca*. 155° *vs* 173-174°) implying that the bromine analogue **2a** delivers more robust halogen bonds compared to **1a**. The polymorph **2b** crystallizes in the triclinic *P*-1 crystal system and has two complexes in the asymmetric unit (See Supporting Information, Figure S1). First moiety contains anisobidendate nitrates in *syn*-mode, and the second in *anti*-mode. Interestingly, the structure shows two types of XBs. First, the complex unit in *syn*-mode forms XBs to a nitrate of an adjacent unit in *anti*-mode *via* both its C2-bromines (C2–Br2···O12 and C2a–Br2a···O12, R_{XB} values are 0.94 and 0.92, respectively). Secondly, two *anti*-mode units, generated by symmetry, are paired against each other by two type II halogen-halogen contacts *via* both C2-bromines (C2b–Br2b···Br2c' and C2c–Br2c···Br2b', both R_{XB} = 0.94) and, furthermore, a type I Br2c···Br2c' contact [*d*(Br2c···Br2c') = 3.313(2) Å]. Another interesting aspect of the Cu(II)-complexes of 2-bromopyridines is their tendency to have short C–Br···Cu distances (see Figure 4a, red dotted lines). This occurs between the Cu(II)-cation acting as a Lewis acid and the nucleophilic region of the C2-bromine which lies orthogonally to the C–Br bond. Similar C–X···Cu interactions have been reported earlier in [Cu(2,5-dihalopyridine)$_2$X$_2$] (X = Cl, Br) complexes by us[21,22] and e.g. Awwadi *et al*.[42] The C–Br···Cu distances in **2a** are 3.18 and 3.35 Å, and thus show significant asymmetry, whereas the respective interatomic distances in the two crystallographically independent complex units in **2b** fall within a more narrow range of 3.23 - 3.25 Å and 3.27 - 3.33 Å. These C–Br···Cu contact distances are on average

longer compared to the [Cu(2,5-dihalopyridine)$_2$X$_2$] complexes in which the polarization of the bromide is larger due to the electron withdrawing C5-halogen and the Cu(II)-cation is affected by the halide nucleophiles at the coordination sphere.

2-Iodopyridine **3** gives only one type of structure (**3a**) with Cu(NO$_3$)$_2$ regardless of crystallization conditions used. Complex **3a** has an orthorhombic crystal system (*Pbcn*) with a half of a molecule in the asymmetric unit in which the anisobidentate nitrates adopt the *syn*-mode. The ligands are not planar in respect to the C2–N1–N1'–C2' dihedral angle but tilt to a very similar ligand conformation like on complex **2a**. However, whereas in **2a** the *syn*-arranged C2-bromines induce a 1-D XB pattern, complex moieties in **3a** are ordered in XB mediated 2-D sheets along the *ab*-plane (Figure 4b). This arises from the two C2–I2···O3 halogen bonds that are formed to anisobidentate nitrate anions of two separate complexes (R_{XB} = 0.88). The Cu(II)-bound nitrate anions of adjacent molecules are within vdW distance to each other [d(N···O)$_2$ = 3.025(3) Å] thus generating a NO_3^-···NO_3^- stacking pattern between coplanar nitrates. The NO_3^-···NO_3^- close contacts were also observed in **2a** but with the corresponding nitrates in a more perpendicular arrangement [d(N···O) = 2.851(8) Å, ∠(N3-O2a-N2') = 148.3°]. The electrophilic nature of central nitrogen in nitrate anion has been previously discussed by Frontera and Bauzá co-workers, who have also investigated the role of π-hole interactions in nitro-functionalized compounds.[43,44] They showed that the charge distribution of NO_3^- is anisotropic and an electropositive region emerges on the N-atom when the nitrate binds to Lewis acids, such

as H_2O and Li^+. In this light, the $NO_3^-\cdots NO_3^-$ contacts observed between Cu(II)-coordinated nitrates are not merely caused due to molecular packing but driven closer as an attractive donor-acceptor interaction.

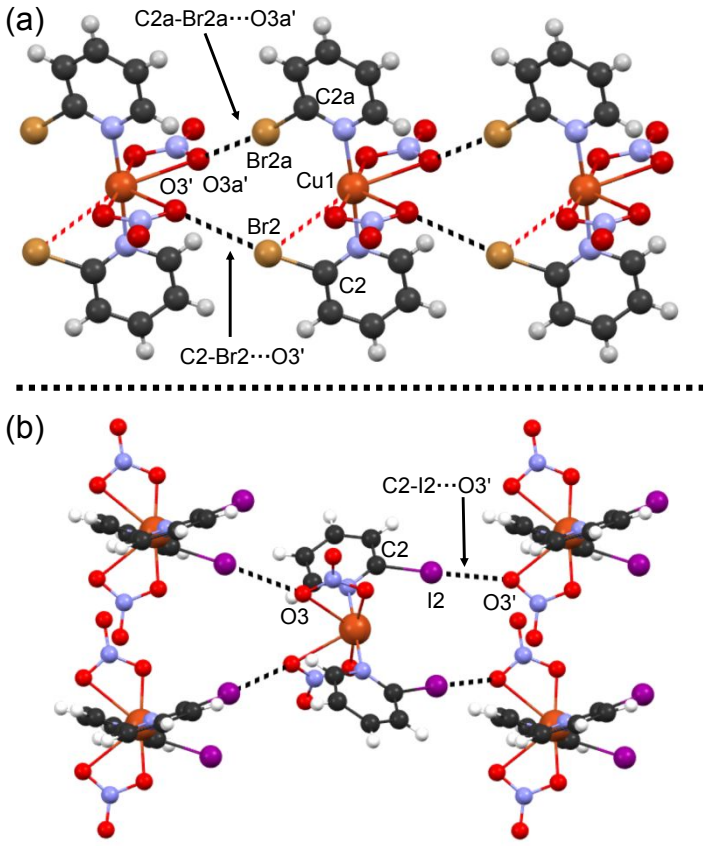

Figure 4. Partial view of molecular packing in crystal structures of complexes a) **2a** and b) **3a** displaying XB interactions. Selected atoms are numbered for the viewing clarity. See Supporting Information Figure S1 for complex **2b**. Atoms labelled with O3' in **2a** and **3a** were generated by using symmetry operators x, -1+y, z and -½+x, -½+y, ½-z, respectively.

3-Halopyridines **4** and **5**, in ACN gave solvated complexes **4a** and **5a**, respectively, whereas crystallization in EtOH resulted in solvent free structures **4b** and **5b**. Both **4a** and **5a** crystallize in the monoclinic crystal system (space groups $P2_1/c$ and $P2_1/n$, respectively) with a single Cu(II)-complex moiety in the asymmetric unit. Furthermore, an acetonitrile molecule is coordinated to the Cu(II)-centre which thereby exhibits pentagonal bipyramid geometry as discussed earlier. Solvent free complexes **4b** and **5b** crystallize in the triclinic crystal system *P*-1 and have half of a complex in their corresponding asymmetric units. Both structures show somewhat less distorted octahedral geometries compared to **4a** and **5a** due to the more centric binding of the equatorial bidentate nitrates that is allowed by the lack of steric hindrance between the organic halogens and the nitrate anions. It can also be noted that these non-solvated complexes have the 3-halopyridines in coplanar arrangement whereas the solvent adducts **4a** and **5a** have the pyridine ligands closer to perpendicular conformation (*ca*. 113.0° and 97.6° dihedral C2–N1–N1a–C2a angles).

The C3-chlorines in **4a** are XB passive and molecular packing is mainly arranged *via* face-to-face π-π packing with both 3-chloropyridine groups, NO_3^-···C≡N anion-π contacts [*d*(C7–O2) = 3.035(4) Å] and by NO_3^-···H–C interactions between nitrates and $_{(3Clpy)}$C–H as well as the methyl end of the coordinated acetonitrile molecule (Figure 5a). Similarly, in **4b** the C3-chlorines are also XB passive and, in addition to NO_3^-···H–C interactions, intermolecular N–O···π contacts occur between adjacent nitrate and carbons of C3-

chlorines in pyridine ligands [*d*(N2–O2···C2" = 3.076(4), *d*(N2–O2···C3" = 3.088(4)] (Figure 5b).

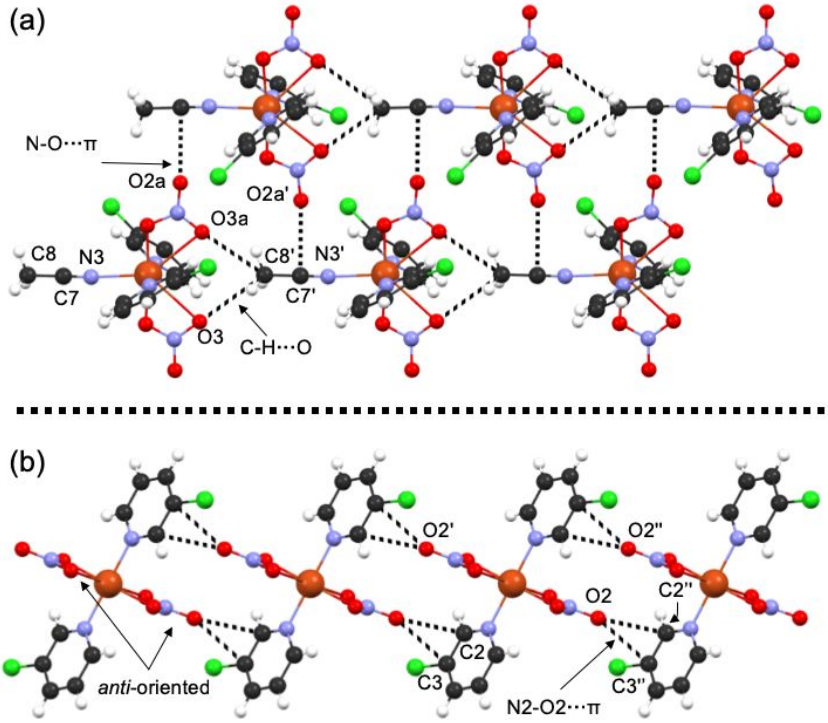

Figure 5. Partial packing view of (a) **4a** and (b) **4b** displaying HBs and N–O···π interactions. Selected atoms are numbered for viewing clarity. Atoms labelled with C8' in **2a,** and C3'' in **3a**, were generated by using symmetry operators x, -1+y, z and 1-x, 2-y, 1-z, respectively.

Complex **5a** shows similarities but also some significant differences in its molecular packing compared to **4a** owing to the stronger XB donor group. In **5a**, one of the two C3-bromines is XB active and binds to an adjacent nitrate anion (R_{XB} = 0.96). The XB passive C3-bromine is electrostatically driven towards the adjacent XB active C3-bromine to a distance which is barely above the vdW radius, but geometrically shows the characteristics

of a type II halogen-halogen contact. The discrete repeating units are interconnected by similar motifs found in **4a**. These include NO_3^-···H–C interactions between aryl/methyl C–H and nitrates as well as NO_3^-···C≡N anion-π contacts [*d*(C7–O2) = 3.113(4) Å; Figure 6a]. As shown in Figure 6b, the crystallographically equal C3-bromines of **5b** are XB active (R_{XB} = 0.98) and yield a linear 1-D halogen bond chain in the direction of *c*-axis of the unit cell. The C3–Br3···O–N bond distances in **5a** and **5b** are similar and indicate that the Cu(II)-cation induced polarization of the 3-bromopyridine ring is not significantly affected by the inclusion of the ACN molecule to the Cu(II) coordination sphere. In the crystal lattice, the complexes are connected *via* several weak C–H···O–N, N–O···π(C3), and N–O···π(C2) interactions. It can be noted that the nitrate anions adopt *syn*-mode both in **4a** and **5a** due to ACN coordination, while solvent-free Cu(II)-centres in **4b** and **5b** have their nitrates in *anti*-mode.

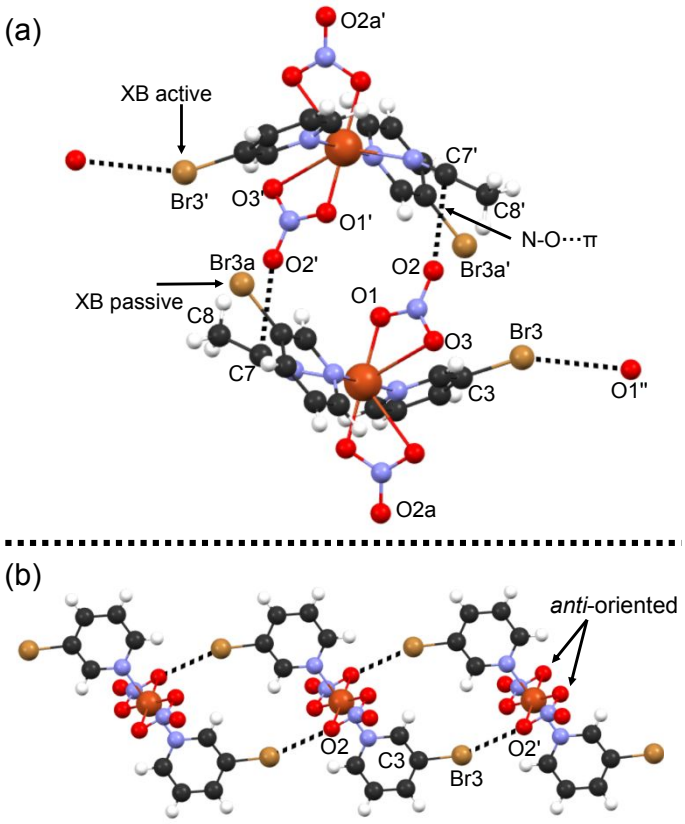

Figure 6. Molecular packing in crystal structures of complexes (a) **5a** and (b) **5b** displaying XBs and anion-π interactions. Selected atoms are numbered for viewing clarity. Atoms labelled with O2' in **5a** and **5b** were generated by using symmetry operators 1-x, 1-y, 1-z and -x, 1-y, 2-z, respectively.

3-Iodopyridine (**6)** is clearly an exception to the examined *mono*-substituted halopyridine series as it is the only ligand forming a 1-D coordination polymer regardless of crystallization conditions (Table 1). The complex **6a** crystallizes in the monoclinic system ($P2_1/n$) and its asymmetric unit consists of one and a half of 2:1 halopyridine-$Cu(NO_3)_2$ moieties: two crystallographically independent copper(II) atoms (one of which lies on inversion centre) and three 3-iodopyridine and nitrate groups (Figure 7). The

intramolecular interactions, that orientate the pyridine ligands within the polymer chains, consist of perpendicular $NO_3^-\cdots NO_3^-$ type short contacts [*d*(N4···O3a) = 2.913(5) Å] and 3-iodopyridine π-stacks along the crystallographic *a*-axis. In contrast, halogen bonds seemingly play an important role in determining the intermolecular polymer-polymer interactions. The monodentate nitrate anion forms the shortest XB (R_{XB} = 0.87), followed by the bridging bis-monodentate nitrate (R_{XB} = 0.92) and bridging mono- and bidentate-nitrates (R_{XB} = 0.99). Although the R_{XB} parameter is not necessarily a reliable indicator of the XB strength, the observed R_{XB} values correlate with the degree of depletion of the negative charge density from nitrate anions to the Cu(II)-cations (*i.e.* the number of Cu–O bonds per nitrate). In coplanar mode, XB is formed between O-atom and the XB donor, whereas in perpendicular orientation the acceptor moiety is more likely the π-system of the NO_3^- anion. In the latter mode, repulsion between the nucleophilic region of the XB donor atom and the nitrate is higher than in coplanar orientation.

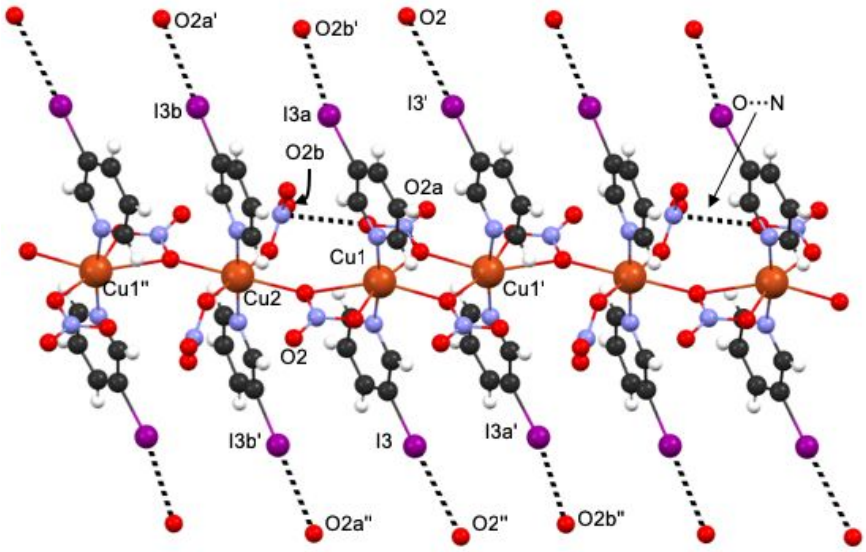

Figure 7. Partial packing view of 1-D polymeric structure of **6a**. Selected atoms are numbered for viewing clarity.

All three 4-halopyridine complexes crystallize from ACN as solvates (**7a**, **8a** and **9a**) regardless of mixing ratio. From EtOH, 4-chloro- and 4-bromopyridines yield solvent free complexes (**7b** and **8b)** whereas with 4-iodopyridine EtOH adduct (**9b**) is formed. Complexes **7a**, **8a** and **9a** are crystallographically isostructural and crystallize in the monoclinic crystal system ($P2_1/n$). Analogously to other solvated structures (*vide supra*), the asymmetric unit consists of a Cu(II)-centre that is surrounded by two 4-halopyridine ligands, two anisobidentate nitrate anions in *syn*-mode, and one ACN molecule, thereby resulting in a pentagonal bipyramid geometry. The ACN adduct structures **7a**, **8a** and **9a** reveal $(NO_3^-)_2\cdots H_3C–C\equiv N$ motifs, similar to ones in **4a** and **5a**, wherein the N–O···C–C≡N contact distances range between *ca*. 3.07 Å and 3.23 Å. All three complexes have XB active halogens showing perpendicular C4–X4···π(O–NO_2^-) XBs as shown in Figures 8a, 8b and 9a. The comparison between the two systems, **1a** and **7a**, in which the C–Cl act as XB donors shows that the R_{XB} values for C4–Cl4···O–N XBs are higher compared to C2–Cl2···O–N XBs whereas the C–Cl···O angle in **7a** (177.1° *vs* 155.1° for **7a** and **1a**, respectively) fulfils the XB directional criteria better. The shorter XB distance in **1a** could be explained by the *ortho*-substituents showing stronger resonance (+R) effect than *para*-substituents in pyridines, and by the interplay of the attractive σ-hole (C4–Cl4)···π(O–NO_2^-) interaction and the repulsion between the orthogonally oriented nitrate π-electrons and

the electron rich region of the Cl-atom around the σ-hole (in **1a** the nitrate is coplanar to the XB donor which minimizes the repulsive interaction).

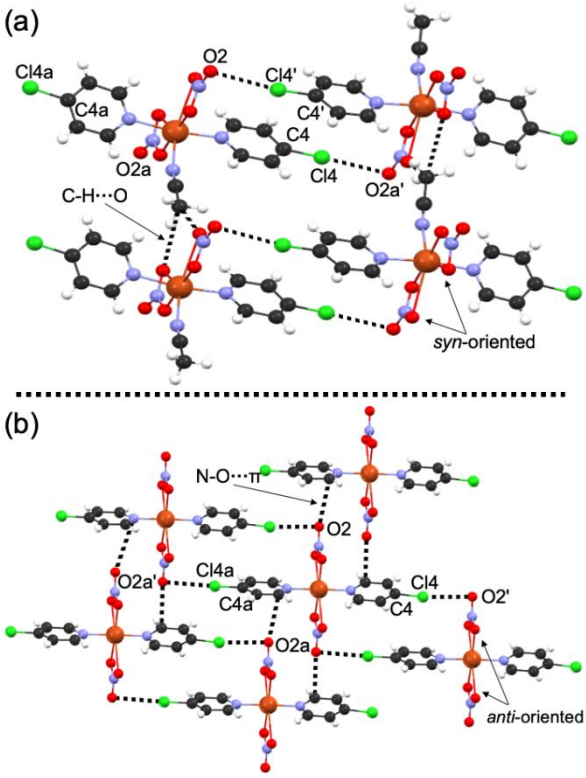

Figure 8. Partial view of molecular packing displaying XB, anion-π and O···H–C short contacts in (a) **7a** and (b) **7b**. Selected atoms are numbered for viewing clarity. Atoms labelled with O2a' in **7a** and **7b** were generated by using symmetry operators ½+x, 1.5-y, -½+z and x, y, -1+z, respectively.

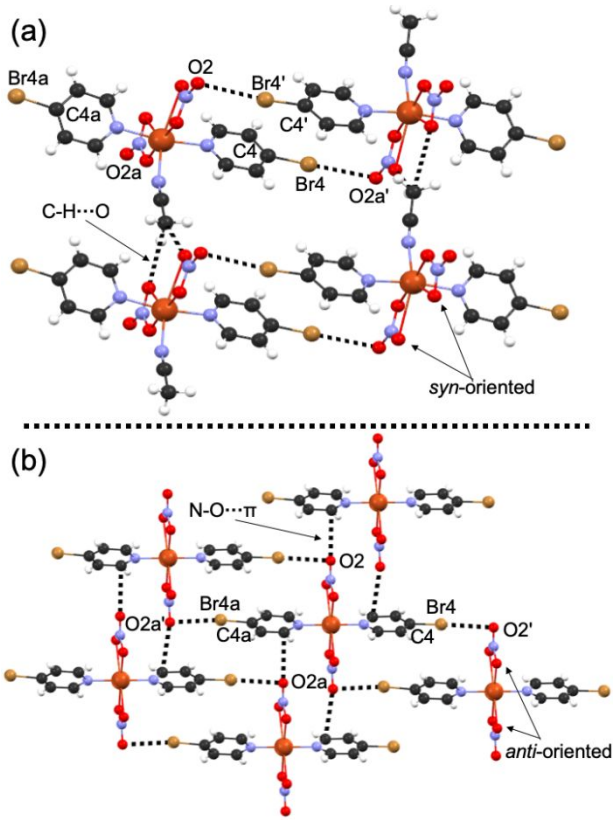

Figure 9. Partial view of molecular packing displaying XB, anion-π and O···H–C short contacts in (a) **8a** and (b) **8b**. Selected atoms are numbered for viewing clarity. Atoms labelled with O2a' in **8a** and **8b** were generated by using symmetry operators ½+x, 1½-y, -½+z and x, y, -1+z, respectively.

The complexes **7b** and **8b** are isostructural and crystallize in the triclinic system (*P*-1) with distorted octahedral geometry and nitrate anions occupying the equatorial positions, as shown in Figures 8b and 9b. Similarly to ACN adduct complexes, the adjacent complex moieties in **7b** and **8b** have similar perpendicular C4–X4···π(O–NO_2^-) XBs between C4-halogens and *anti*-mode nitrate anions [R_{XB}(**7b**) = 0.96, 0.98; R_{XB}(**8b**) = 0.92, 0.93]. In addition, the nitrate anions show an intricate interplay of other weak intermolecular

interactions. Firstly, the nitrates of adjacent complex units are coplanar with the respective O- and N-atoms within the vdW vicinity. Furthermore, the nitrates are connected by edge-to-face N–O···π(C2) interactions to the halopyridine rings which leads to the formation of 2-D sheet type structures (Figure 8b and 9b).

Contrary to **7b** and **8b**, complex **9b** crystallizes as an EtOH solvate having EtOH coordinated to the Cu(II)-centre. The triclinic (*P*-1) crystal structure has repeating units that are formed from HB dimers [graph set R2,2(8)][45] which further assemble into a larger layer-like network through C4–I4···O–N XBs (Figure 10b). Similarly to ACN solvates, adjacent complex units show a $(NO_3^-)_2$···H_3C–CH_2–OH motif which arises from the interaction between *syn*-mode nitrate oxygens and methyl-carbon of EtOH. The "bifurcated" $(NO_3)_2$···methyl motifs are thus present in all studied solvated structures assisting Cu(II)-complexes to yield robust supramolecular structures. A Cambridge Structural Database (CSD)[48] search for $M(NO_3)_2$···methyl motifs revealed a total of 23 hits, of which 10 structures (remaining ones are polymorphs) have either terminal or M–O bound oxygen atoms that manifest short contacts with the methyl groups of solvents such as acetonitrile, methanol and ether.

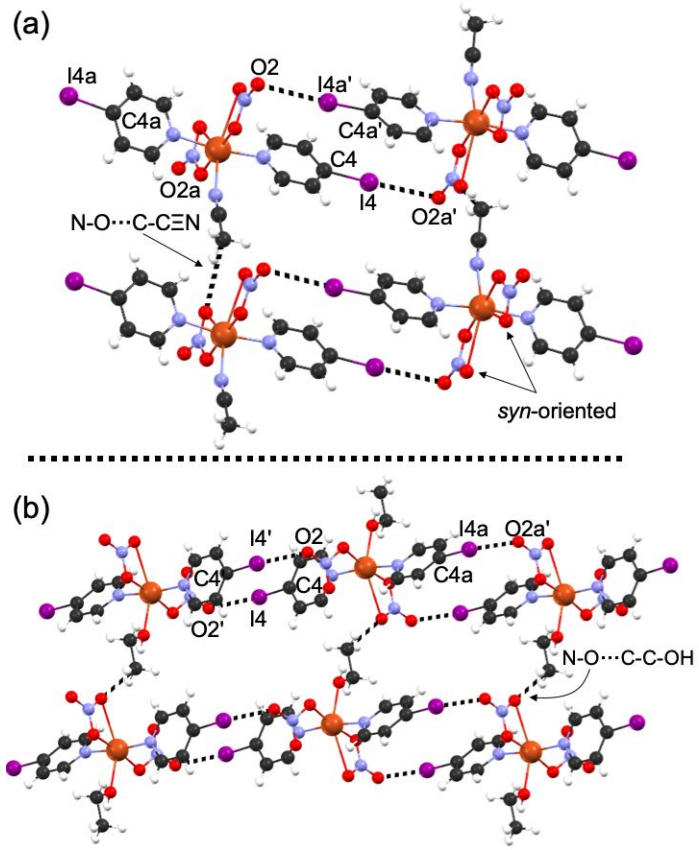

Figure 10. Section of 3-D crystal packing displaying short contacts in (a) **9a** and (b) **9b**. Selected atoms are numbered for viewing clarity. Atoms labelled with I4a' in **8a** and **8b** were generated by using symmetry operators -½+x, ½-y, ½+z and -x, -y, -z, respectively.

Lastly some of the structural trends observed in the studied [Cu(*n*-halopyridine)$_2$(NO$_3$)$_2$] complexes will be summarized briefly. The steric hinderance by C2-halogens in [Cu(2-halopyridine)$_2$(NO$_3$)$_2$] effectively prevent any solvent coordination to the Cu(II)-centre while in other [Cu(3/4-halopyridine)$_2$(NO$_3$)$_2$], the inclusion of solvent at the Cu(II)-geometry may be controlled by the selection of solvent (Figure 11a-c). The halogen bonds in 2- and 3-chloropyridines are too weak to be observed in solid-state X-ray crystal

structures, potentially disrupted or dominated by other interactions during molecular packing to yield stable crystal lattices. In contrast, the remainder of the *n*-halopyridines show systematic formation of XB interactions as intended, generally occurring between the covalently bound halogen, thus acting as the XB donor, and Cu(II)-bound NO_3^- group as XB-acceptor. According to the R_{XB} value, which can be taken as a coarse estimate of the XB strength, the position of the halogen atom in the ring does not significantly alter the XB donor properties of the organo-halogens. Of special note, 4-halopyridines consistently generate very similar XB arrangements regardless of the halogen type or Cu(II) coordination environment (Figure 11d-f). The prevalence of other non-covalent interactions that originate from the use NO_3^- anions was unexpected. The speculated π-hole on the Cu(II)-coordinated NO_3^- and the consequent $NO_3^-\cdots NO_3^-$ interactions could be identified in 5 out of 10 structures, none of which were solvates. Moreover, the $Cu(NO_3)_2\cdots H_3C$ motifs are ubiquitous in the solvated structures. The PI values listed in Table 2 have small range (69.4 - 73.8%), and the addition of solvent to the Cu(II)-centre decreases the PI only by *ca*. 2-4% whereas the packing efficacies between the polymorphic structure show no systematic difference.

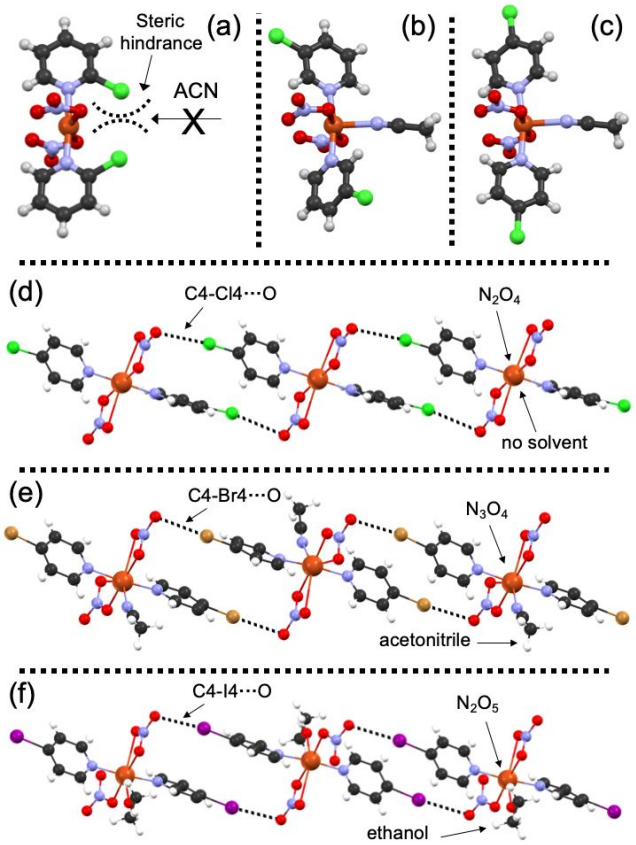

Figure 11. Comparison of (a-c) steric hindrance using [Cu(*n*-chloropyridine)$(NO_3)_2$] complexes (*n* = 2, 3 and 4) and (d-f) copper(II) coordination spheres and XB interactions in solvated [Cu(4-halopyridine)$(NO_3)_2$] complexes.

CONCLUSIONS

C–X···O–N halogen bonding in fifteen [Cu(*n*-halopyridine)$(NO_3)_2$] (*n* = 2, 3, 4) complexes obtained by mixing nine *n*-halopyridines with $Cu(NO_3)_2$ in 1:1 or 2:1 ratio in either ACN or EtOH were systematically studied. In twelve of the fifteen complexes halogen bonds could be assigned between the nitrate and halopyridine. The calculated normalized halogen bond distance parameter (R_{XB}) values between 0.88 and 0.99 suggest that the C–X···O–N

halogen bonds differ slightly in strength, and in some systems contribute significantly to the overall molecular packing scheme. Whereas in others, their overall impact is smaller. Despite of nitrate anion's versatile coordination modes and flexibility of Cu(II) coordination geometry, all complexes prefer the formation of discrete 2:1 ligand to metal stoichiometry in their X-ray crystal structures. The most commonly observed coordination mode for the nitrate anions was anisobidentate, wherein one of the O–Cu contact distances was some 0.3 – 0.6 Å longer than the other ones. Cu(II)-complexes of *n*-halopyridines afforded by crystallization from ethanol were all solvent-free with the exception of 4-iodopyridine, which resulted in EtOH molecule coordinated to the copper(II)-centre. Despite of high coordination affinity of acetonitrile towards Cu(II), discrete acetonitrile adducts were observed only in case of 3-halopyridine and 4-halopyridine complexes. The [Cu(2-halopyridine)$(NO_3)_2$] complexes crystallized from acetonitrile contain no solvent in their copper(II) coordination spheres due to bulky C2-halogens around Cu(II)-center. In the absence of halogen bonds, such as in the case of acetonitrile bound [Cu(3-chloropyridine)$(NO_3)_2$] complex, N–O···Me–C≡N and N–O···π(C≡N) interactions provide stability to the crystal lattice. Also, a $(NO_3)_2$···methyl motif was identified in all of the solvated complexes, suggesting their significant role in the molecular arrangement of Cu(II) complexes and further applicability as a crystal engineering tool.

EXPERIMENTAL SECTION

General information: All solvents used for crystal growth were reagent grade and are used as received without further purification. The ligands, 2-chloropyridine (**1**), 2-bromopyridine (**2**), 2-iodopyridine (**3**), 3-chloropyridine (**4**), 3-bromopyridine (**5**), 3-iodopyridine (**6**), 4-chloropyridine (**7**), 4-bromopyridine hydrochloride (**8**·HCl) and 4-iodopyridine hydrochloride (**9**·HCl) were purchased from TCI Chemicals Europe, and $Cu(NO_3)_2{\cdot}3H_2O$ from Sigma Aldrich.

General crystallization procedure:

Synthesis of complexes 1a to 6a: To a solution of $Cu(NO_3)_2{\cdot}3H_2O$ (0.062 mmol) in acetonitrile/ethanol (1.0 ml), was added halopyridine (0.062 mmol or 0.124 mmol) dissolved in acetonitrile/ethanol (0.5 ml) at room temperature. Slow evaporation of corresponding solutions resulted in single crystals suitable for X-ray diffraction analysis.

Synthesis of 7a to 9b: 4-halopyridine hydrochloride (0.074 mmol or 0.136 mmol) dissolved in 1:1 chloroform:water (1.0 ml) solutions were neutralized using 10% NaOH solution. The organic layers were separated and added to $Cu(NO_3)_2{\cdot}3H_2O$ (0.062 mmol) in acetonitrile/ethanol (1.0 ml). The solutions were subjected to slow evaporation to give single crystals suitable for X-ray diffraction analysis.

Crystal structure determination: The X-ray single crystal data and experimental details for data collections are given in Supporting Information Table S1-S4. Single-crystal X-ray

data for all complexes, except **2a**, were measured using a Bruker-Nonius Kappa CCD diffractometer equipped with an APEX-II CCD detector and graphite-monochromated Mo-Kα (λ = 0.71073 Å) radiation. The data for **2a** were collected using a Rigaku SuperNova single-source Oxford diffractometer with an EoS CCD detector and multi-layer optics monochromated Mo-Kα (λ = 0.71073 Å) radiation. The data collection and reduction for **2a** were performed using the program *CrysAlisPro*[47] and Gaussian face-index absorption correction method was applied. [47] The data obtained by Bruker Nonius Kappa diffractometer were processed using the program COLLECT[48] and HKL DENZO AND SCALEPACK, [49] and the absorption correction of intensities were made using SADABS[50] with multi-scan absorption correction type method. All structures were solved with direct methods (*SHELXS*) [51,52] and refined by full-matrix least squares on F^2 using the *OLEX2* software, [53] which utilizes the *SHELXL*-2013[51,52] module.

ASSOCIATED CONTENT

Supporting Information. The Supporting Information is available free of charge on the ACS Publication website at DOI: XXXXX. Synthesis of metal complexes, X-ray experimental details and powder X-ray diffraction data are included in the Supporting Information.

ACKNOWLEDGMENT

The authors gratefully acknowledge financial support from the Academy of Finland (RP: grant no. 298817, ML: grant no. 277250 and AP: grant no. 315911) and the University of Jyväskylä.

REFERENCES

(1) Troff, R. W.; Mäkelä, T.; Topić, F.; Valkonen, A.; Raatikainen, K.; Rissanen, K. *European J. Org. Chem.* **2013**, *2013*, 1617–1637.

(2) Gilday, L. C.; Robinson, S. W.; Barendt, T. A.; Langton, M. J.; Mullaney, B. R.; Beer, P. D. *Chem. Rev.* **2015**, *115*, 7118–7195.

(3) Mukherjee, A.; Tothadi, S.; Desiraju, G. R. *Acc. Chem. Res.* **2014**, *47*, 2514–2524.

(4) Li, B.; Zang, S.-Q.; Wang, L.-Y.; Mak, T. C. W. *Coord. Chem. Rev.* **2016**, *308* (Part 1), 1–21.

(5) Aakeröy, C. B.; Baldrighi, M.; Desper, J.; Metrangolo, P.; Resnati, G. *Chem. – A Eur. J.* **2013**, *19*, 16240–16247.

(6) Beale, T. M.; Chudzinski, M. G.; Sarwar, M. G.; Taylor, M. S. *Chem. Soc. Rev.* **2013**, *42*, 1667–1680.

(7) Erdelyi, M. *Chem. Soc. Rev.* **2012**, *41*, 3547–3557.

(8) Cavallo, G.; Metrangolo, P.; Milani, R.; Pilati, T.; Priimagi, A.; Resnati, G.; Terraneo, G. *Chem. Rev.* **2016**, *116*, 2478–2601.

(9) Awwadi, F. F.; Haddad, S. F.; Turnbull, M. M.; Landee, C. P.; Willett, R. D. *CrystEngComm* **2013**, *15*, 3111–3118.

(10) Ohno, T.; Nakabayashi, K.; Imoto, K.; Komine, M.; Chorazy, S.; Ohkoshi, S.

CrystEngComm **2018**, *20*, 7236–7241.

(11) Fourmigué, M.; Batail, P. *Chem. Rev.* **2004**, *104*, 5379–5418.

(12) Imakubo, T.; Sawa, H.; Kato, R. *J. Chem. Soc. Chem. Commun.* **1995**, 16, 1667–1668.

(13) Laguna, A.; Lasanta, T.; López-de-Luzuriaga, J. M.; Monge, M.; Naumov, P.; Olmos, M. E. *J. Am. Chem. Soc.* **2010**, *132*, 456–457.

(14) Mahmudov, K. T.; Kopylovich, M. N.; Guedes da Silva, M. F. C.; Pombeiro, A. J. L. *Coord. Chem. Rev.* **2017**, *345*, 54–72.

(15) Awwadi, F. F.; Willett, R. D.; Peterson, K. A.; Twamley, B. *Chem. – A Eur. J.* **2006**, *12*, 8952–8960.

(16) Zordan, F.; Brammer, L. *Cryst. Growth Des.* **2006**, *6*, 1374–1379.

(17) Zordan, F.; Brammer, L.; Sherwood, P. *J. Am. Chem. Soc.* **2005**, *127*, 5979–5989.

(18) Brammer, L. *Chem. Soc. Rev.* **2004**, *33*, 476–489.

(19) Brammer, L.; Minguez Espallargas, G.; Libri, S. *CrystEngComm* **2008**, *10*, 1712–1727.

(20) Awwadi, F. F.; Turnbull, M. M.; Alwahsh, M. I.; Haddad, S. F. *New J. Chem.* **2018**, *42*, 10642–10650.

(21) Puttreddy, R.; von Essen, C.; Peuronen, A.; Lahtinen, M.; Rissanen, K. *CrystEngComm* **2018**, *20*, 1954–1959.

(22) Puttreddy, R.; von Essen, C.; Rissanen, K. *Eur. J. Inorg. Chem.* **2018**, *2018*, 2393–2398.

(23) Borovina, M.; Kodrin, I.; Đaković, M. *CrystEngComm* **2018**, *20*, 539–549.

(24) Topić, F.; Puttreddy, R.; Rautiainen, J. M.; Tuononen, H. M.; Rissanen, K.

CrystEngComm **2017**, *19*, 4960–4963.

(25) Puttreddy, R.; Topić, F.; Valkonen, A.; Rissanen, K. *Crystals* **2017**, *7*, 214.

(26) Puttreddy, R.; Jurček, O.; Bhowmik, S.; Mäkelä, T.; Rissanen, K. *Chem. Commun.* **2016**, *52*, 2338–2341.

(27) Takezawa, H.; Murase, T.; Resnati, G.; Metrangolo, P.; Fujita, M. *Angew. Chemie Int. Ed.* **2015**, *54*, 8411–8414.

(28) Deane, P. O.; Guthrie-strachan, J. J.; Kaye, P. T.; Whittaker, R. E. *Synth. Commun.* **2011**, 37–41.

(29) Morozov, I. V; Serezhkin, V. N.; Troyanov, S. I. *Russ. Chem. Bull.* **2008**, *57*, 439–450.

(30) Bravin, C.; Badetti, E.; Puttreddy, R.; Pan, F.; Rissanen, K.; Licini, G.; Zonta, C. *Chem. - A Eur. J.* **2018,** *24*, 2936–2943.

(31) All attempts to obtain single crystals using ligand **7** and Cu(II) salt in 1:1 molar ratio from ethanol were unsuccessful. Nonetheless, the unit cell parameters deduced from corresponding PXRD experiment indicate that the crystal structure of the resulted complex is most likely similar to that of **7b** crystallized in 2:1 ratio from ethanol.

(32) Albada, G. A. van; Mutikainen, I.; Turpeinen, U.; Reedijk, J. *Acta Crystallogr. Sect. E* **2002**, *58*, m55–m57.

(33) Xuan, R.; Li, M.; Wan, Y. *Acta Crystallogr. Sect. C* **2003**, *59*, m462–m464.

(34) Torelli, S.; Belle, C.; Gautier-Luneau, I.; Pierre, J. L.; Saint-Aman, E.; Latour, J. M.; Le Pape, L.; Luneau, D. *Inorg. Chem.* **2000**, *39*, 3526–3536.

(35) Butcher, R. J.; Tesema, Y. T.; Yisgedu, T. B.; Gultneh, Y. *Acta Crystallogr. Sect. E* **2008**, *64*, m233–m234.

(36) Dong, Y.-B.; Cheng, J.-Y.; Wang, H.-Y.; Huang, R.-Q.; Tang, B.; Smith, M. D.; zur Loye, H.-C. *Chem. Mater.* **2003**, *15*, 2593–2604.

(37) Ribelli, T. G.; Wahidur Rahaman, S. M.; Daran, J.-C.; Krys, P.; Matyjaszewski, K.; Poli, R. *Macromolecules* **2016**, *49*, 7749–7757.

(38) Concia, A. L.; Beccia, M. R.; Orio, M.; Ferre, F. T.; Scarpellini, M.; Biaso, F.; Guigliarelli, B.; Réglier, M.; Simaan, A. J. *Inorg. Chem.* **2017**, *56*, 1023–1026.

(39) Spek, A. L. *Acta Crystallogr. Sect. D* **2009**, *65*, 148–155.

(40) Mukherjee, A.; Desiraju, G. R. *IUCrJ* **2014**, *1*, 49–60.

(41) Frontera, A. *Coord. Chem. Rev.* **2013**, *257*, 1716–1727.

(42) Awwadi, F. F.; Willett, R. D.; Twamley, B.; Turnbull, M. M.; Landee, C. P. *Cryst. Growth Des.* **2015**, *15*, 3746–3754.

(43) Bauzá, A.; Frontera, A.; Mooibroek, T. J. *Nat. Commun.* **2017**, *8*, 14522.

(44) Bauzá, A.; Sharko, A. V; Senchyk, G. A.; Rusanov, E. B.; Frontera, A.; Domasevitch, K. V. *CrystEngComm* **2017**, *19*, 1933–1937.

(45) Etter, M. C.; MacDonald, J. C.; Bernstein, J. *Acta Crystallogr. Sect. B* **1990**, *46*, 256–262.

(46) The Cambridge Structural Database, *Version 5.40* (last upated, February. 2019).

(47) *Rigaku Oxford Diffraction. 2018. Version 1.171.38.43.*

(48) *Bruker AXS BV, Madison, WI, USA; 1997–2004*.

(49) Otwinowski, Z.; Minor, W. In *Macromolecular Crystallography Part A*; Methods Enzymology, Charles W. Carter, Jr.; Sweet R. M., Editors.; Academic Press, 1997; Volume 276, 307–326.

(50) Blessing, R. H. *J. Appl. Crystallogr.* **1997**, *30*, 421–426.

(51) Sheldrick, G. M. *Acta Crystallogr. Sect. A* **2008**, *64*, 112–122.

(52) Sheldrick, G. M. *Acta Crystallogr. Sect. C* **2015**, *71*, 3–8.

(53) Dolomanov, O. V; Bourhis, L. J.; Gildea, R. J.; Howard, J. A. K.; Puschmann, H. *J. Appl. Crystallogr.* **2009**, *42*, 339–341.

FOR TABLE OF CONTENTS USE ONLY

Metal-bound Nitrate Anion as an Acceptor for Halogen Bonds in *mono*-Halopyridine-Copper(II) nitrate Complexes

Rakesh Puttreddy,[a] Anssi Peuronen,[b] Manu Lahtinen[a] and Kari Rissanen[a]*

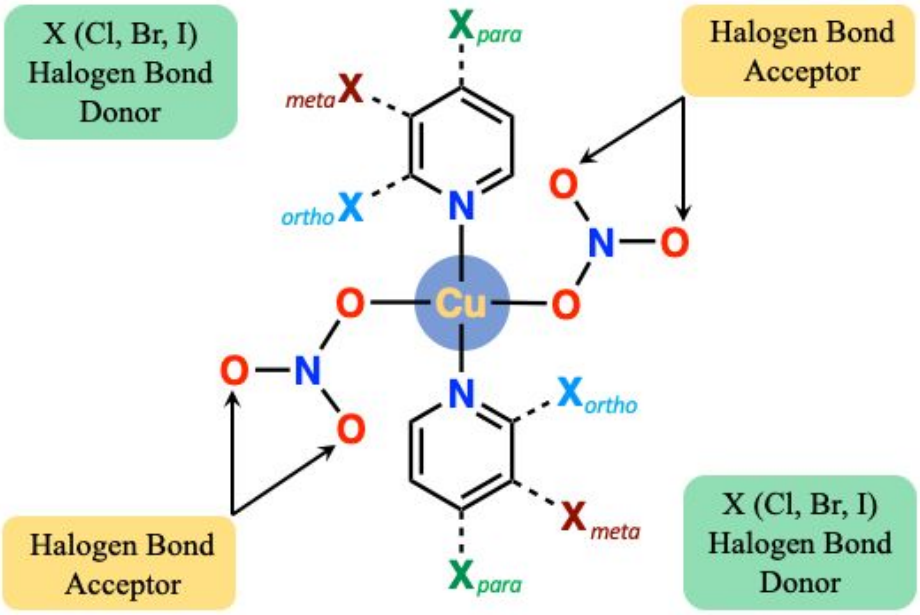

Three series of *mono*-substituted halopyridine-$Cu(NO_3)_2$ complexes are studied for C−X···O−N halogen bonds between Cu(II) bound nitrate anion oxygen and halogens on the core pyridine rings.